

Heteronuclear J cross-polarisation in liquids using amplitude and phase modulated mixing sequences

Anika Kirschstein · Christian Herbst · Kerstin Riedel ·
Michela Carella · Jörg Leppert · Oliver Ohlenschläger ·
Matthias Görlach · Ramadurai Ramachandran

Received: 28 November 2007 / Accepted: 3 March 2008 / Published online: 1 April 2008
© Springer Science+Business Media B.V. 2008

Abstract The design of mixing sequences for heteronuclear J cross-polarisation in the liquid state has been examined employing supercycles of amplitude/phase modulated RF pulses. The Fourier coefficients defining the modulation profiles of the pulses were optimised numerically so as to achieve efficient magnetisation transfer within the desired range of resonance offsets. A variety of supercycles, pulsewidths and RF field strengths were considered in implementing heteronuclear anisotropic and isotropic mixing sequences. The coherence transfer characteristics of the sequences obtained were evaluated by numerical simulations. The experimental performances of the sequences were tested by measurements carried out on a moderate sized protein at 750 MHz. The results presented demonstrate that the approach adopted in this study can be employed effectively to tailor, as per the experimental requirements and constraints, the RF-field modulation profiles of the pulses constituting the mixing scheme for generating heteronuclear J cross-polarisation sequences.

Keywords Heteronuclear cross-polarization ·
Scalar couplings · Numerical design ·
Amplitude and phase modulated RF pulse sequences

Introduction

Mixing periods leading to in-phase, scalar coupling mediated heteronuclear Hartmann-Hahn (HH) coherence

transfers (Glaser et al. 1996) form an important building block in many of the RF pulse sequences employed in biomolecular solution state NMR spectroscopy (Wüthrich 1986), e.g. for resonance assignments in proteins (Majumdar et al. 1993) and nucleic acids (Simorre et al. 1996). Compared to a refocussed INEPT step (Ernst et al. 1987) leading to anti-phase coherence transfers, heteronuclear HH mixing schemes have been found to have many advantages, including a better tolerance to RF field inhomogeneity (Majumdar et al. 1995) and the possibility to suppress exchange-broadening effects (Krishnan et al. 1995; Mueller et al. 1995). In uniformly ^{13}C labelled biomolecular systems, unlike the situation with refocussed INEPT, the possibility also exists for ^{13}C – ^{13}C homonuclear HH transfers (Glaser et al. 1996) during heteronuclear ^{13}C – ^1H HH mixing. Such magnetisation transfers can be exploited in realising sensitivity improvements in biomolecular NMR experiments, as demonstrated in obtaining through-bond ^1H – ^{13}C – ^{13}C – ^1H side-chain correlations in proteins via the ^1H – ^{13}C – ^{13}C – ^1H -TOCSY pulse scheme (Majumdar et al. 1993). In the context of protein resonance assignments, heteronuclear HH type mixing schemes have also been successfully applied to induce magnetisation transfers even in homonuclear spin systems involving a large isotropic chemical shift difference between scalar coupled nuclei, as in $^{13}\text{C}^\alpha$ – $^{13}\text{C}'$ and $^{13}\text{C}^\beta$ – $^{13}\text{C}^{\text{arom}}$ cases (Zuiderweg et al. 1996; Carlomagno et al. 1996). Heteronuclear HH mixing can be employed to achieve the transfer of either one or both transverse magnetisation components (Glaser et al. 1996) and either over the same (Glaser et al. 1996) or different (Carlomagno et al. 1997) spectral widths in the two dimensions. A variety of heteronuclear HH multiple-pulse sequences involving the application of rectangular (Glaser et al. 1996), both windowless and windowed, as well as shaped RF pulse schemes

A. Kirschstein · C. Herbst · K. Riedel · M. Carella · J. Leppert ·
O. Ohlenschläger · M. Görlach · R. Ramachandran (✉)
Research group Biomolecular NMR spectroscopy, Leibniz
Institute for Age Research, Fritz Lipmann Institute, 07745 Jena,
Germany
e-mail: raman@fli-leibniz.de

(Zuiderweg et al. 1996; Carlomagno et al. 1996) have been reported in the literature. In this work we have examined the possibility to design different types of heteronuclear HH mixing schemes via a general approach involving the parametrisation of the RF field profile of the pulses constituting the mixing scheme in terms of a Fourier series. To obtain the desired transfer characteristics, the Fourier coefficients were numerically optimised taking into account the experimental requirements and constraints such as the range of coupling strengths, isotropic chemical shift separation between the nuclei involved in the coherence transfer, as in $^{13}\text{C}^\alpha/^{13}\text{C}'$ and $^{13}\text{C}^\beta/^{13}\text{C}^{\text{arom}}$ cases, resonance offset range in the two dimension and the limits, if any, on the RF field strength employed. The results from these investigations are presented below.

Numerical and experimental procedures

A heteronuclear two spin 1/2 system was considered in designing cross-polarisation sequences that were implemented as supercycles of amplitude/phase modulated RF pulses. The Hamiltonian in the doubly rotating-frame during RF irradiation is given by

$$H = 2\pi \delta_1 I_{1z} + 2\pi \delta_2 I_{2z} + 2\pi J_{12} I_{1z} I_{2z} + \omega_{11}(t) \{I_{1x} \cos \phi_1(t) + I_{1y} \sin \phi_1(t)\} + \omega_{12}(t) \{I_{2x} \cos \phi_2(t) + I_{2y} \sin \phi_2(t)\}. \quad (1)$$

The phase $\{\varphi(t)\}$ and amplitude $\{v_1(t)\}$ modulation profiles of a pulse are expressed as Fourier series (Geen et al. 1991; Paepe et al. 2003; Abramovich et al. 1995):

$$\{\phi(t)\} = a_0 + \sum a_n \cos(n\omega t) + \sum b_n \sin(n\omega t); \quad (2)$$

$$\{v_1(t)\} = C \{c_0 + \sum c_n \cos(n\omega t) + \sum d_n \sin(n\omega t)\}, \quad (3)$$

where $\omega = 2\pi/t_p$ is the modulation frequency, t_p is the pulse duration and C is a constant set to 10 kHz in our case. Unless mentioned otherwise, our studies were typically carried out considering only a cosine Fourier series. Neglecting B_1 field inhomogeneities, the Fourier coefficients were numerically optimised in order to obtain efficient magnetisation transfers over the desired range of resonance offsets δ_1 and δ_2 . The downhill simplex method of Nelder and Mead (Press et al. 1985) was used to minimise the error function

$$\varepsilon(a_0, a_n, c_0, c_n) = \sum_{\delta_1, \delta_2} \varepsilon_J(a_0, a_n, c_0, c_n, \delta_1, \delta_2) + \varepsilon_{\text{rms}}. \quad (4)$$

ε_{rms} is a penalty function that is employed to avoid the root mean square of the RF field strength, $B_1(\text{rms})$, exceeding a pre-set value. During optimisation, the value of ε_{rms} was

either set to zero or to a large value, depending on whether the calculated value of $B_1(\text{rms})$ for a given amplitude modulation profile was found, respectively, to be less than or greater than the desired upper limit of $B_1(\text{rms})$. In the design of anisotropic heteronuclear HH sequences that permit the transfer of only one transverse component (Glaser et al. 1996) the amount of x magnetisation transferred to the second spin $\langle I_{2x} \rangle$ is calculated at $\tau_{\text{mix}} = 1/(J_{12})$, starting with $\langle I_{1x} \rangle = 1$ and $\langle I_{2x} \rangle = 0$ at zero mixing time. The error term ε_J was set to $[1 - \langle I_{2x} \rangle]$ during the course of the optimisation. Isotropic heteronuclear HH sequences (Glaser et al. 1996) were designed by monitoring the efficacies of the sequences for simultaneous transfer of more than one magnetisation component. In our case, starting with $\langle I_{1z} \rangle = 1$ and $\langle I_{2z} \rangle = 0$ at $\tau_{\text{mix}} = 0$, $\varepsilon_{Jz} = [1 - \langle I_{2z} \rangle]$ at $\tau_{\text{mix}} = 3/(2J_{12})$ was calculated. In addition, starting with $\langle I_{1x} \rangle = 1$ and $\langle I_{2x} \rangle = 0$ at $\tau_{\text{mix}} = 0$, $\varepsilon_{Jx} = [1 - \langle I_{2x} \rangle]$ was also calculated at $\tau_{\text{mix}} = 3/(2J_{12})$. To eventually arrive at the best possible optimised RF field profiles, $\varepsilon(a_0, a_n, c_0, c_n)$ was calculated at every stage of the optimisation using either ε_{Jz} or ε_{Jx} , depending, respectively, whether $\varepsilon_{Jz} > \varepsilon_{Jx}$ or $\varepsilon_{Jx} > \varepsilon_{Jz}$.

To save computational time the RF pulses were divided only into 100 slices of equal duration. Using well-known phase cycles such as $m16$ (Levitt et al. 1983), $xy16$ (Gullion et al. 1990), appropriate supercycling of the RF pulses was carried out for generating mixing sequences. Unless mentioned otherwise, sequences were typically designed by setting the starting Fourier coefficients to zero. In general, it was possible to generate sequences with satisfactory performance characteristics with a limited number of Fourier coefficients in the range of 6–8. Increasing the number of coefficients did not lead to significant improvements. Typical values of $\{^{13}\text{C}/^{15}\text{N}\}^{-1}\text{H}$, $^{13}\text{C}^\alpha\text{-}^{13}\text{C}'$ and $^{13}\text{C}^\beta\text{-}^{13}\text{C}^{\text{arom}}$ scalar coupling strengths, RF pulses with durations in the range of 100–900 μs and representative rms field strengths were considered, with no restrictions imposed on the peak RF field strength. Calculations were carried out using computer programs written in-house for Zeeman field strengths corresponding to a ^1H resonance frequency of either 800 or 600 MHz. RF pulse sequences were tested experimentally using a ~ 1 mM (^{13}C , ^{15}N)-labelled sample of a 154 amino acid heat stable protein from *Methanobacterium thermoautotrophicum* (in D_2O at pH 7.0 and 318 K; Carella 2008). Experiments were carried out on a 750 MHz Varian INOVA NMR spectrometer equipped with pulse field gradient accessories, waveform generators and a triple resonance probe, employing the same number of slices per pulse as in the numerical calculations. No significant improvements were seen via numerical simulations by using more than 100 slices, e.g. 1,000 slices. The States procedure was used for quadrature detection in the indirect dimension (States et al.

1982). Proton chemical shifts were referenced to the H₂O signal relative to DSS and ¹³C chemical shifts were referenced to external dioxane/H₂O.

Results and discussion

Mixing sequences were designed by first fixing the values for the scalar coupling and Zeeman field strengths, the bandwidths in the two dimensions and the limits, if any, on the rms/peak RF field strength. Depending on the RF pulsewidth, the mixing sequence was implemented using an appropriate supercycle. Computations were carried out to obtain the desired transfer characteristics, respectively, at $\tau_{\text{mix}} = 1/(J_{12})$ or $3/(2J_{12})$ in the anisotropic and isotropic cases. In finding a satisfactory solution for a given situation, several optimisation runs were generally carried out starting with RF pulses of different durations. Initial calculations were done using the same amplitude modulated RF field profile on both channels and such an approach was often found to be sufficient for generating anisotropic mixing sequences. Only in situations where better performance is found to be required, other RF field modulation profiles were examined, e.g. phase-modulated RF pulse schemes or two different amplitude modulated RF pulse schemes on the two channels. The potential of the method for generating efficient heteronuclear mixing sequences was assessed by considering a few representative cases. The Fourier coefficients, RF-field profiles (Fig. 1) and the coherence transfer characteristics of some of the sequences obtained are presented below.

Figure 2 shows the performance characteristics of some of the heteronuclear anisotropic mixing sequences, AK_n-JCH_{aniso1}. These sequences involve the application of the same amplitude modulated RF pulse schemes on both channels. They were generated with no restrictions imposed on the peak RF field strength and considering an upper limit of 10 kHz for the rms field strength on the two channels, a bandwidth of ± 12 kHz in both the dimensions and using different scalar coupling strengths given in the figure caption. Figure 2a shows the *x* to *x* magnetisation transfer efficiency of the AK1-JCH_{aniso1} sequence generated with $J_{\text{CH}} = 140$ Hz, an RF pulse of 450 μs duration and *m16* supercycle, requiring a peak RF field strength of 18 kHz. The performance of the AK2-JCH_{aniso1} sequence generated with $J_{\text{CH}} = 140$ Hz, an RF pulse of 300 μs duration and *m12* (corresponding to the first 12 elements of *m16*) supercycle is shown in Fig. 2b. This sequence requires a peak RF field strength of 25 kHz with an rms value of ~ 8.2 kHz. Figure 2c and d show the performances of the AK3-JCH_{aniso1} and AK4-JCH_{aniso1} sequences generated considering a scalar coupling strength of 160 and 106 Hz, respectively. For comparison, Fig. 2e

mixing scheme	c_0	c_1	c_2	c_3	c_4	c_5
AK1-JCH _{aniso1} (<i>m16</i>)	0.287	0.309	-0.443	0.496	-0.686	-0.907
AK2-JCH _{aniso1} (<i>m12</i>)	0.111	-0.429	0.222	-0.460	0.3464	-0.862
AK3-JCH _{aniso1} (<i>m16</i>)	-0.422	0.250	0.392	-0.984	0.582	-0.328

mixing scheme	c_0	c_1	c_2	c_3	c_4	c_5
AK4-JCH _{aniso1} (<i>m16</i>)	-0.472	0.464	0.126	-0.936	0.192	-0.280
	d_1	d_2	d_3	d_4	d_5	d_6
	-0.478	0.320	0.311	0.206	-0.151	-0.209

mixing scheme	a_0	a_1	a_2	a_3	a_4	a_5
AK1-JCH _{iso} (<i>xy16</i>)	-26.4	4.9	16.5	-22.5	14.1	17.1
AK2-JCH _{iso} (<i>m16</i>)	-54.7	-37.8	-3.3	17.7	26.8	-12.2

mixing scheme	c_0	c_1	c_2	c_3	c_4	c_5
AK1-JCH _{aniso2} (<i>m12</i>) H	-0.141	-1.024	0.041	0.235	0.151	-0.904
AK1-JCH _{aniso2} (<i>m12</i>) C	-0.145	-0.968	-0.034	0.377	0.162	-0.918
AK2-JCH _{aniso2} (<i>m12</i>) H	-0.083	-0.812	0.272	0.512	0.205	-0.477
AK2-JCH _{aniso2} (<i>m12</i>) C	-0.075	-0.780	0.253	0.378	0.064	-0.666

mixing scheme	c_0	c_1	c_2	c_3	c_4	c_5	c_6	c_7	c_8
AK1-JC ⁹⁰ C ^{aniso} (<i>m16</i>)	0.136	-0.216	-0.168	-0.185	0.217	-0.110	0.232	-0.846	0.0
AK2-JC ⁹⁰ C ^{aniso} (<i>m16</i>)	0.008	0.011	-0.308	-0.030	0.161	0.044	-0.581	0.0	0.0
AK3-JC ⁹⁰ C ^{aniso} (<i>m16</i>)	-0.017	-0.363	0.035	-0.165	0.001	-0.047	-0.121	-0.836	0.0
AK4-JC ⁹⁰ C ^{aniso} (<i>m12</i>)	-0.033	0.011	0.013	-0.384	-0.058	0.187	0.057	-0.663	0.0
AK1-JC ^β C ^{arom} (<i>m16</i>)	-0.085	-0.278	0.384	-0.272	-0.672	0.461	0.0	0.0	0.0
AK2-JC ^β C ^{arom} (<i>m12</i>)	0.121	0.0	0.0	0.0	0.068	0.149	-0.323	-0.132	-0.405
AK3-JC ^β C ^{arom} (<i>m16</i>)	-0.117	-0.347	0.241	0.345	-0.180	-0.208	0.698	-0.302	0.0
AK4-JC ^β C ^{arom} (<i>m16</i>)	-0.024	0.0	0.0	0.0	-0.419	0.008	0.177	0.030	-0.539

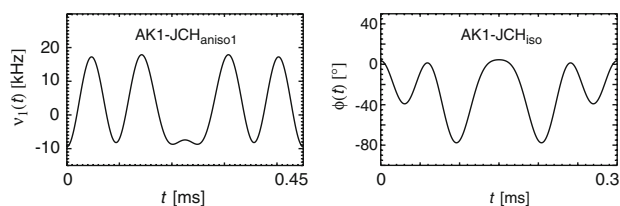


Fig. 1 The Fourier coefficients (a_0 [°], a_n [°], c_0 , c_n , d_n) and the supercycling (*m16*: 0°, 0°, 180°, 180°, 0°, 180°, 180°, 0°, 180°, 180°, 0°, 180°, 180°, 0°, 0°, 180°; *m12*: 0°, 0°, 180°, 180°, 0°, 180°, 180°, 0°, 180°, 180°, 0°, 0°; *xy16*: 0°, 90°, 0°, 90°, 90°, 0°, 90°, 0°, 180°, 270°, 180°, 270°, 270°, 180°, 270°, 180°) employed in different heteronuclear HH mixing schemes. The modulation profiles of the RF pulses in two representative mixing schemes are also given

and f show the performance observed with the DIPSI-2 (Shaka et al. 1988) and the MGS-1 (Schwendinger et al. 1994; Glaser et al. 1996) sequences, respectively. It is worth mentioning that, with an rms field strength of 10 kHz, the MGS-2 sequence (Schwendinger et al. 1994) has a better performance characteristic than the MGS-1 sequence. However, the MGS-2 sequence requires a peak

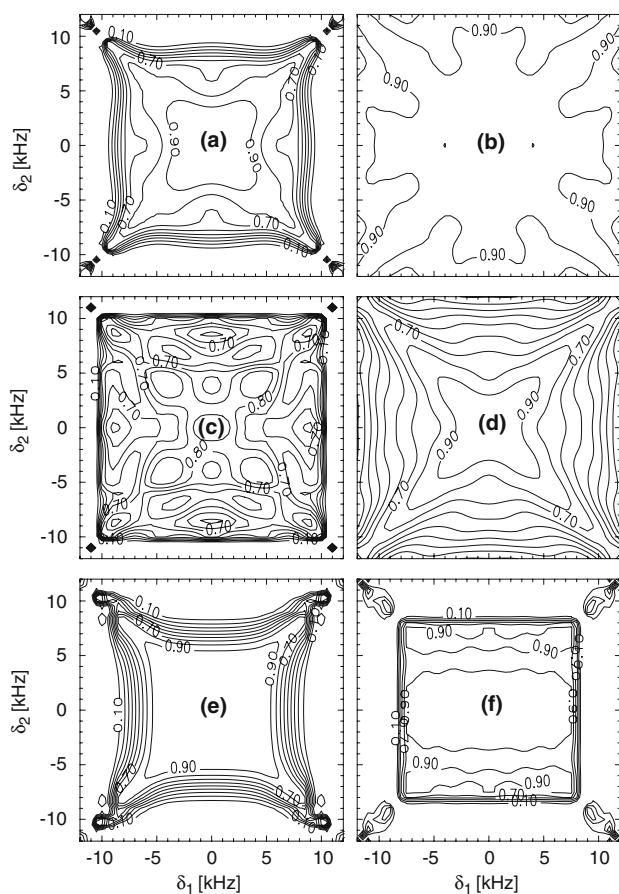


Fig. 2 x to x magnetisation transfer efficiencies of different heteronuclear HH mixing schemes monitored at $\tau_{\text{mix}} \sim 1/(J_{12})$ with (a) AK1-JCH_{aniso1}, $J_{\text{CH}} = 140$ Hz, 450 μs RF pulse and $m16$ supercycle, (b) AK2-JCH_{aniso1}, $J_{\text{CH}} = 140$ Hz, 300 μs RF pulse duration and $m12$ supercycle, (c) AK3-JCH_{aniso1}, $J_{\text{CH}} = 160$ Hz, 400 μs RF pulse, $m16$ supercycle, 22 kHz peak (10 kHz rms) field strength, (d) AK4-JCH_{aniso1}, $J_{\text{CH}} = 106$ Hz, 300 μs RF pulse, $m16$ supercycle, 22 kHz peak (10 kHz rms) field strength, (e) DIPSI-2 with an RF field strength of 10 kHz, $J_{\text{CH}} = 100$ Hz, and $m4$ supercycle (f) MGS-1 with an rms field strength of 10 kHz (peak 27 kHz), $J_{\text{CH}} = 111$ Hz and $m8$ supercycle. Except for AK4-JCH_{aniso1}, all other sequences were generated considering only a cosine Fourier series

RF field strength of 30 kHz. With peak RF field strengths requirements in the range of 27–30 kHz, we have been also able to generate sequences with better performance characteristics than MGS-2 (data not shown). However, since high peak RF field strengths are not typically available experimentally, we have not considered such sequences in this work.

Figure 3 shows the performance characteristics of some of the isotropic mixing sequences, AK n -JCH_{iso}, involving the application of the same phase modulated RF pulse schemes on both channels. The transfer characteristics of the AK1-JCH_{iso} and AK2-JCH_{iso} sequences are shown in Fig. 3a and b and Fig. 3c and d, respectively. These were generated considering a RF field strength of 10 kHz, a magnetisation transfer bandwidth of ± 5 kHz in both the

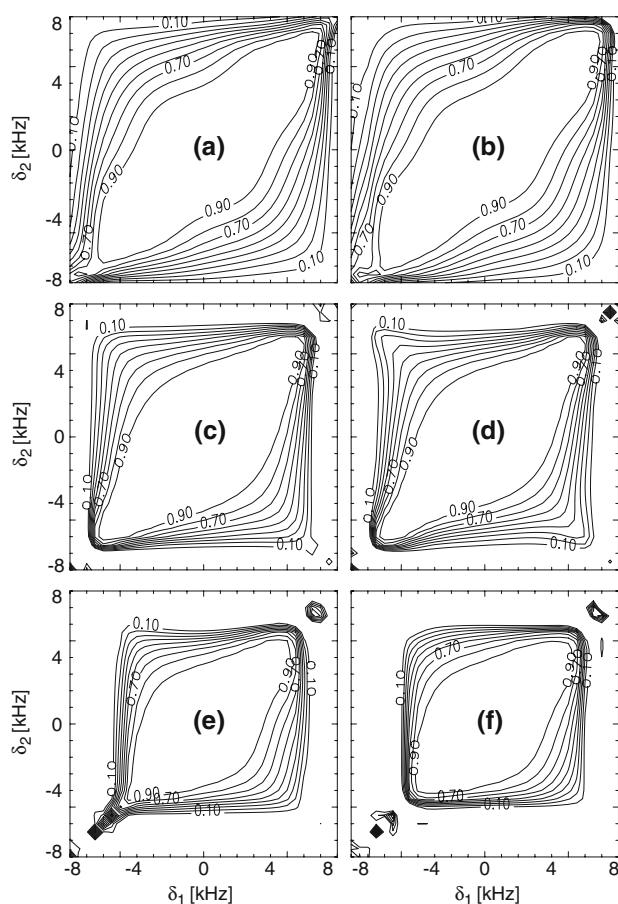


Fig. 3 x to x (a, c, e) and y to y (b, d, f) magnetisation transfer efficiencies of different heteronuclear HH isotropic mixing schemes monitored at $\tau_{\text{mix}} \sim 3/(2J_{12})$ with (a, b) AK1-JCH_{iso}, $J_{\text{CH}} = 102$ Hz, 300 μs RF pulse and $xy16$ supercycle, (c, d) AK2-JCH_{iso}, $J_{\text{CH}} = 104$ Hz, 450 μs RF pulse, $m16$ supercycle and (e, f) JESTER-1, $J_{\text{CH}} = 106$ Hz and $m16$ supercycle

dimensions and J_{CH} of ~ 100 Hz. For comparison, the x to x and y to y magnetisation transfer efficiencies of the JESTER-1 (Glaser et al. 1996) sequence are also given in Fig. 3e and f. The plots in Fig. 3 demonstrate the possibilities for obtaining isotropic mixing sequences with improved performance characteristics using phase modulated RF pulses. Figure 4 shows the magnetisation transfer characteristics of the anisotropic mixing sequences, AK n -JCH_{aniso2}, involving the application of two different amplitude modulated RF pulse schemes on the two channels. The sequences AK1-JCH_{aniso2} (Fig. 4a) and AK2-JCH_{aniso2} (Fig. 4b), requiring a peak RF field strength of 18 and 16 kHz, respectively, were designed to realise a magnetisation transfer bandwidths of ± 3 and ± 6 kHz in the two dimensions. A scalar coupling strength of 120 and 106 Hz, RF pulses with durations of 350 and 400 μs and an upper limit for the rms field strength of 10 and 8 kHz, respectively, were used in generating these sequences. The AK1-JCH_{aniso2} sequence was obtained using the Fourier

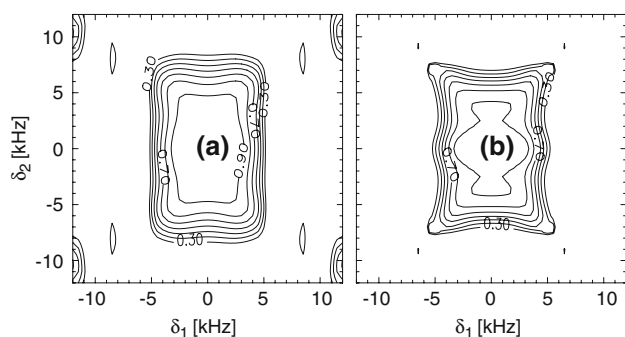


Fig. 4 x to x magnetisation transfer characteristics of the anisotropic heteronuclear HH mixing sequences (a) AK1-JCH_{ano2}, $J_{CH} = 120$ Hz, 350 μ s RF pulse, $m12$ supercycle, 18 kHz peak (10 kHz rms) field strength (b) AK2-JCH_{ano2}, $J_{CH} = 106$ Hz, 400 μ s RF pulse, $m12$ supercycle, 16 kHz peak (8 kHz rms) field strength

coefficients of one of the heteronuclear anisotropic mixing sequences (data not shown) as the starting Fourier coefficients on the ^{13}C channel. The starting Fourier coefficients on the ^1H channel were set to zero. The Fourier coefficients of the AK1-JCH_{ano2} sequence was employed as the starting point for generating the AK2-JCH_{ano2} sequence via local optimisation. These plots demonstrate that it is equally possible to tailor the coherence transfer bandwidth characteristics by employing two different RF-field modulated pulse schemes on the two channels.

Figure 5 shows the performance of some of the purely amplitude modulated anisotropic mixing sequences, AKn-JCC_{ano}, that were designed to achieve magnetisation transfers in homonuclear ^{13}C spin systems with large isotropic chemical shift separation, $\Delta\delta_{\text{iso}}$, between the scalar coupled nuclei such as $^{13}\text{C}^\alpha$ - $^{13}\text{C}'$ and $^{13}\text{C}^\beta$ - $^{13}\text{C}^{\text{arom}}$. Keeping the ^{13}C carrier at $(\Delta\delta_{\text{iso}}/2)$ and setting the starting Fourier coefficients to zero, optimisation runs were carried out considering a homonuclear two spin rotating frame Hamiltonian with the full $2\pi J_{12}I_1 \cdot I_2$ scalar coupling term, $\Delta\delta_{\text{iso}}$ values of 120 ($\text{C}^\alpha/\text{C}'$) and 100 ppm ($\text{C}^\beta/\text{C}^{\text{arom}}$), Zeeman field strengths corresponding to a ^1H frequency of 600 and 800 MHz, $J_{\text{C}^\alpha\text{C}'}$ and $J_{\text{C}^\beta\text{C}^{\text{arom}}}$, respectively, of 55 and 50 Hz, magnetisation transfer bandwidths of ± 2 kHz in both the dimensions and an upper limit on the rms field strength in the range of 4–7 kHz. As in the heteronuclear case, the amount of x magnetisation transferred to the second spin $\langle I_{2x} \rangle$ is calculated at $\tau_{\text{mix}} = 1/(J_{12})$, starting with $\langle I_{1x} \rangle = 1$ and $\langle I_{2x} \rangle = 0$ at zero mixing time. It is generally difficult to achieve efficient magnetisation transfer between scalar coupled nuclei with large $\Delta\delta_{\text{iso}}$ values using broadband, homonuclear ^{13}C - ^{13}C isotropic mixing sequences. However, even in such situations the plots shown in Fig. 5 demonstrate that the approach outlined here can be conveniently applied for designing

anisotropic cross-polarisation sequences taking into account the experimental requirements.

The performance of some of the heteronuclear mixing schemes reported here were also tested experimentally. Figure 6 shows the 2D ^{13}C - ^1H HSQC spectra of the (^{13}C , ^{15}N)-labelled 154 a.a heat stable protein sample obtained using the mixing schemes mentioned in the figure caption. The experimental performances of the sequences are found to be satisfactory, in agreement with the results from numerical simulations. In addition to the signals arising from one bond ^{13}C - ^1H correlations, cross-peaks arising from homonuclear magnetisation transfers during heteronuclear mixing are also seen. Although mixing sequences were numerically designed considering a particular scalar coupling strength, the performances of these sequences are found to be not extremely sensitive to minor variations in the coupling strength, as reflected by the good cross-peak intensities seen in the entire aliphatic $^{13}\text{C}/^1\text{H}$ spectral range. Adopting a procedure similar to that employed in this study, the possibilities for implementing homonuclear broadband scalar coupling mediated ^{13}C - ^{13}C and cross-relaxation suppressed ^1H - ^1H isotropic mixing sequences using amplitude and phase modulated RF pulse schemes were recently demonstrated (Kirschstein et al. 2008a, b). The results presented here clearly indicate that the method is equally applicable for designing different heteronuclear HH sequences needed in biomolecular NMR investigations.

Since high field instruments are commonly available and there is ever increasing improvements in the spectrometer hardware, e.g. RF power handling capabilities of the probes, we believe that it will be beneficial to employ mixing schemes that are tailor-made to a given experimental situation. It will not be surprising if such an approach becomes the method of choice in the future, considering the fact that there is ever increasing availability of powerful computational tools. The sequences reported here were developed imposing restrictions on the rms field strength. The optimisation procedure can be adapted, where needed, to develop sequences taking into account restrictions on the peak RF field strength. Additionally, sequences can also be designed to minimise magnetisation transfers in unwanted spectral regions, e.g. in the $^{13}\text{C}^\alpha$ - $^{13}\text{C}^\beta$ region while maximising transfers in the $^{13}\text{C}^\alpha$ - $^{13}\text{C}'$ or $^{13}\text{C}^\beta$ - $^{13}\text{C}^{\text{arom}}$ region. The present study shows that even with a local optimisation procedure, such as the downhill simplex method employed here, and with a simple Fourier representation of the RF-field modulation profiles it is possible to generate (within a short time of a few hours using an HP xw6200 workstation) efficient heteronuclear HH mixing sequences. Although it may be computationally time consuming, it should be possible to generate mixing sequences with improved performance

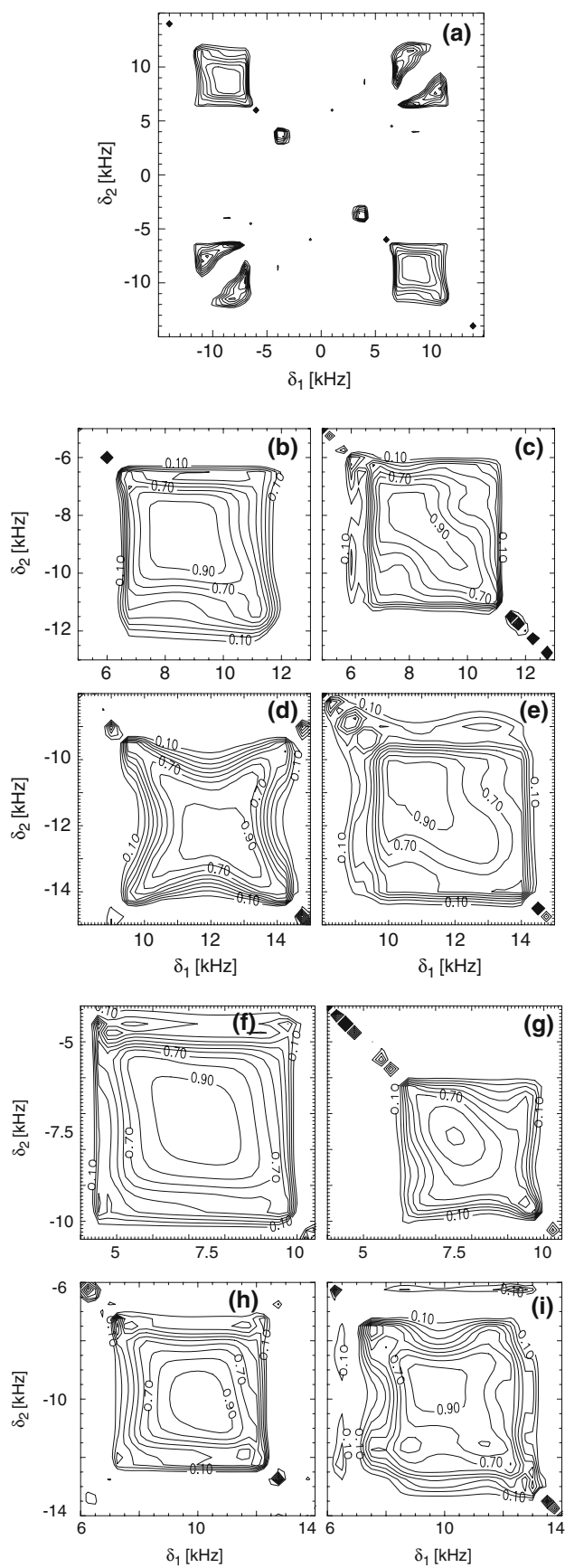


Fig. 5 (a) x to x magnetisation transfer characteristics of the anisotropic mixing sequence AK1-JC $^{\alpha}$ C' $_{\text{aniso}}$, monitored at $\tau_{\text{mix}} \sim 1/(J_{\text{cc}})$ and designed for a homonuclear ^{13}C spin systems with large isotropic chemical shift separation, $\Delta\delta_{\text{iso}}$, between the scalar coupled nuclei. The sequence was generated considering a $\Delta\delta_{\text{iso}}$ value of ± 9 kHz and involves a $m16$ supercycle of an amplitude modulated RF pulse of $570 \mu\text{s}$ duration with 17 kHz peak (7 kHz rms) field strength. The expanded plot of one of the cross-peak regions in the data generated with different sequences are given in b–i. (b) AK1-JC $^{\alpha}$ C' $_{\text{aniso}}$, $\Delta\delta_{\text{iso}} = \pm 9$ kHz, $570 \mu\text{s}$ RF pulse, $m16$ supercycle, 17 kHz peak (7 kHz rms) field strength (c) AK2-JC $^{\alpha}$ C' $_{\text{aniso}}$, $\Delta\delta_{\text{iso}} = \pm 9$ kHz, $560 \mu\text{s}$ RF pulse, $m16$ supercycle, 11 kHz peak (4.8 kHz rms) field strength (d) AK3-JC $^{\alpha}$ C' $_{\text{aniso}}$, $\Delta\delta_{\text{iso}} = \pm 12$ kHz, $570 \mu\text{s}$ RF pulse, $m16$ supercycle, 10 kHz peak (6 kHz rms) field strength (e) AK4-JC $^{\alpha}$ C' $_{\text{aniso}}$, $\Delta\delta_{\text{iso}} = \pm 12$ kHz, $500 \mu\text{s}$ RF pulse, $m12$ supercycle, 12 kHz peak (5.6 kHz rms) field strength (f) AK1-JC $^{\beta}$ C $^{\text{arom}}$ $_{\text{aniso}}$, $\Delta\delta_{\text{iso}} = \pm 7.5$ kHz, $310 \mu\text{s}$ RF pulse, $m16$ supercycle, 14 kHz peak (7.0 kHz rms) field strength (g) AK2-JC $^{\beta}$ C $^{\text{arom}}$ $_{\text{aniso}}$, $\Delta\delta_{\text{iso}} = \pm 7.5$ kHz, $840 \mu\text{s}$ RF pulse, $m12$ supercycle, 8 kHz peak (4.1 kHz rms) field strength (h) AK3-JC $^{\beta}$ C $^{\text{arom}}$ $_{\text{aniso}}$, $\Delta\delta_{\text{iso}} = \pm 10$ kHz, $420 \mu\text{s}$ RF pulse, $m16$ supercycle, 14 kHz peak (7.0 kHz rms) field strength (i) AK4-JC $^{\beta}$ C $^{\text{arom}}$ $_{\text{aniso}}$, $\Delta\delta_{\text{iso}} = \pm 10$ kHz, $620 \mu\text{s}$ RF pulse, $m16$ supercycle and 12 kHz peak (5.0 kHz rms) field strength. These plots were generated considering the full $2\pi J_{12} I_1 \cdot I_2$ scalar coupling term in the simulations

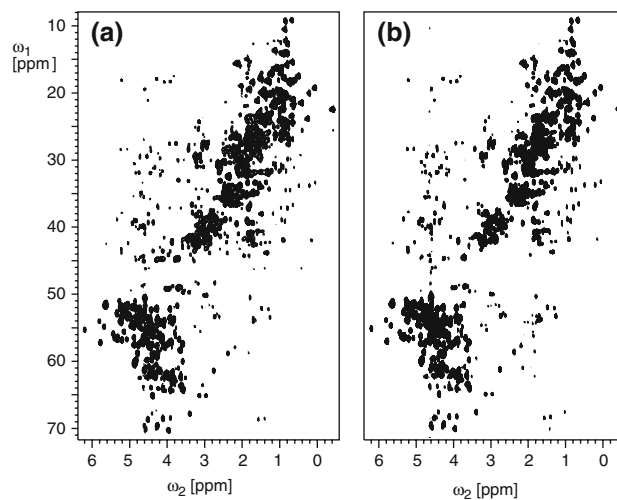


Fig. 6 The 2D ^{13}C - ^1H HSQC spectra of the (^{13}C , ^{15}N)-labelled sample of the 154 amino acid heat stable protein from *Methanobacterium thermoautotrophicum* obtained using a heteronuclear HH mixing step after the t_1 evolution period with the (a) AK1-JCH $_{\text{aniso}1}$ (7.2 ms mix) and (b) AK1-JCH $_{\text{aniso}2}$ (8.4 ms mix) sequences. Recycle time of 1 s, 32 scans per t_1 increment, ^{13}C spectral width of 14 kHz and 256 increments in the indirect ^{13}C dimension were employed with the ^{13}C and ^1H carrier frequencies kept at 40 and 2.5 ppm, respectively

characteristics employing global optimisation procedures, such as simulated annealing (Kirkpatrick et al. 1983) and genetic algorithm (Forrest 1993), and with a better representation of the RF-field modulation profiles.

References

- Abramovich D, Vega S, Quant J, Glaser SJ (1995) The floquet description of TOCSY and E.TACS Y experiments. *J Magn Reson* 115:222–229
- Carella M (2008) Structural characterisation of type-B methionine sulfoxide reductases. PhD thesis, Friedrich-Schiller-Universität Jena
- Carlomagno T, Maurer M, Sattler M, Schwendinger MG, Glaser SJ, Griesinger C (1996) PLUSH TACS Y: Homonuclear planar TACS Y with two-band selective shaped pulses applied to C^α , C' transfer and C^β , C^{aromatic} correlations. *J Biomol NMR* 8:161–170
- Carlomagno T, Luy B, Glaser SJ (1997) “Kin” HEHAHA sequences, heteronuclear Hartmann-Hahn transfer with different bandwidths for spins I and S. *J Magn Reson* 126:110–119
- Ernst RR, Bodenhausen G, Wokaun A (1987) Principles of nuclear magnetic resonance in one and two dimensions. Clarendon Press, Oxford
- Forrest S (1993) Genetic algorithms—principles of natural-selection applied to computation. *Science* 261:872–878
- Geen H, Freeman R (1991) Band-selective radiofrequency pulses. *J Magn Reson* 93:93–141
- Glaser SJ, Quant JJ (1996) Homonuclear and heteronuclear Hartmann-Hahn transfer in isotropic liquids. In: Warren WS (eds) Advances in magnetic and optical resonance. Academic Press, San Diego
- Gullion T, Baker DB, Conradi MS (1990) New, compensated Carr-Purcell sequences. *J Magn Reson* 89:479–484
- Kirkpatrick S, Gelatt CD, Vecchi MP (1983) Optimization by simulated annealing. *Science* 220:671–680
- Kirschstein A (2008a) Amplituden- und phasenmodulierte Mischsequenzen für die Flüssigkeits-NMR-Spektroskopie an Proteinen. Diploma thesis, Friedrich-Schiller-Universität Jena
- Kirschstein A, Herbst C, Riedel K, Carella M, Leppert J, Ohlenschläger O, Görlach M, Ramachandran R (2008b) Broadband homonuclear TOCSY with amplitude and phase-modulated RF mixing schemes. *J Biomol NMR*. doi:1007/s10858-008-9225-7
- Krishnan VV, Rance M (1995) Influence of chemical-exchange among homonuclear spins in heteronuclear coherence-transfer experiments in liquids. *J Magn Reson A* 116:97–106
- Levitt MH, Freeman R, Frenkiel T (1983) Broadband decoupling in high-resolution nuclear magnetic resonance spectroscopy. *Adv Magn Reson* 11:47–110
- Majumdar A, Zuiderweg ERP (1995) Efficiencies of double-resonance and triple-resonance J cross-polarization in multidimensional NMR. *J Magn Reson A* 113:19–31
- Majumdar A, Wang H, Morshausen RC, Zuiderweg ERP (1993) Sensitivity improvement in 2D and 3D HCCH spectroscopy using heteronuclear cross-polarization. *J Biomol NMR* 3:387–397
- Mueller L, Legault P, Pardi A (1995) Improved RNA structure determination by detection of NOE contacts to exchange-broadened amino protons. *J Am Chem Soc* 117:11043–11048
- Paeppe GD, Hodgkinson P, Emsley L (2003) Improved heteronuclear decoupling schemes for solid-state magic angle spinning NMR by direct spectral optimization. *Chem Phys Lett* 376:259–267
- Press WH, Teukolsky SA, Vetterling WT, Flannery BP (1985) Numerical recipes in C. University Press, Cambridge
- Schwendinger MG, Quant J, Schleucher J, et al (1994) Broad-band heteronuclear Hartmann-Hahn sequences. *J Magn Reson A* 111:115–120
- Shaka AJ, Lee CJ, Pines A (1988) Iterative schemes for bilinear operators; application to spin decoupling. *J Magn Reson* 77:274–293
- Simorre JP, Zimmermann GR, Mueller L, Pardi A (1996) Triple-resonance experiments for assignment of adenine base resonances in $^{13}C/^{15}N$ -labeled RNA. *J Am Chem Soc* 118:5316–5317
- States DJ, Haberkorn RA, Ruben DJ (1982) A two-dimensional nuclear Overhauser experiment with pure absorption phase in four quadrants. *J Magn Reson* 48:286–292
- Wüthrich K (1986) NMR of proteins and nucleic acids. John Wiley & Sons, New York, NY
- Zuiderweg ERP, Zeng L, Brutscher B, Morshausen RC (1996) Band-selective hetero- and homonuclear cross-polarization using trains of shaped pulses. *J Biomol NMR* 8:147–160